CHEMISTRY
A EUROPEAN JOURNAL

DOI: 10.1002/chem.200903190

The Squaramide versus Urea Contest for Anion Recognition

Valeria Amendola,[a] Greta Bergamaschi,[a] Massimo Boiocchi,[b] Luigi Fabbrizzi,*[a] and Michele Milani[a]

Abstract: The interaction of a neutral squaramide-based receptor, equipped with two 4-nitrophenyl substituents ($\mathbf{R_{sq}}$), with halides and oxoanions has been studied in MeCN. UV/Vis and ^{1}H NMR spectroscopy titration experiments clearly indicated the formation of 1:1 hydrogen bonding $[\mathbf{R_{sq}}\cdots X]^+$ complexes with all the investigated anions. X-ray diffraction studies on the chloride and bromide complex salts confirmed the 1:1 stoichiometry and indicated the establishment of bifurcated hydrogen-bond interactions between the squaramide-based receptor and the halide anion that involved both 1) amide N–H and 2) aryl proximate C–H fragments, for a total of four bonds. Probably due to the contribution of C–H fragments, complexes of $\mathbf{R_{sq}}$ with halides are 1 to 2 orders of magnitude more stable than the corresponding ones with the analogous urea-based receptor that contains two 4-nitrophenyl substituents ($\mathbf{R_{ur}}$). In the case of oxoanions, $\mathbf{R_{sq}}$ forms complexes, the stability of which decreases with the decreasing basicity of the anion ($H_2PO_4^- > NO_2^- \approx HSO_4^- > NO_3^-$), and is comparable to that of complexes of the urea-based receptor $\mathbf{R_{ur}}$. Such a behaviour is ascribed to the predominance of different contributions: electrostatic interaction for halides, acid-to-base 'frozen' proton transfer for oxoanions. Finally, with the strongly basic anions F^- and CH_3COO^-, $\mathbf{R_{sq}}$ first gives genuine hydrogen-bond complexes of 1:1 stoichiometry; then, upon addition of a second anion equivalent, it undergoes deprotonation of one N–H fragment, with the simultaneous formation of the dianion hydrogen-bond complexes, $[HF_2]^-$ and $[CH_3COOH\cdots CH_3COO]^-$, respectively. In the case of the urea-based derivative $\mathbf{R_{ur}}$, deprotonation takes place with fluoride but not with acetate. The apparently higher Brønsted acidity of $\mathbf{R_{sq}}$ with respect to $\mathbf{R_{ur}}$ reflects the capability of the squaramide receptor to delocalise the negative charge formed on N–H deprotonation over the cyclobutene-1,2-dione ring and the entire molecular framework.

Keywords: acid–base equilibria · anions · charge transfer · hydrogen bonds · pi interactions

Introduction

Anion recognition by artificial host molecules (receptors) is an important topic of supramolecular chemistry.[1] Receptors can be neutral or positively charged. Most neutral artificial receptors establish hydrogen-bonding interactions with the anion by means of N–H fragments from amides,[2] urea/thiourea[3] and pyrroles.[4] Urea in particular is an attractive building block for designing anion receptors because it possesses two N–H fragments, which can bind 1) a single acceptor atom (e.g., that of a halide ion), thus forming a six-membered chelate ring, or 2) two adjacent oxygen atoms of an oxoanion, to give an eight-membered chelate ring. A variety of receptors that contain two or more urea moieties have been synthesised. Examples include cyclic and acyclic systems of varying complexity, arranged for multipoint recognition of anionic guests.[5] Moreover, Hay et al. used the urea subunit as a building block for the computer-aided design of sophisticated receptors for targeted anions of varying geometrical features.[6] It has been recently demonstrated that synthons that contain covalently linked bipyridine and urea fragments, which profit from the template effect of four Ni^{II} ions, self-assemble to encapsulate a sulfate ion in water, thereby forming a complex of unprecedented stability.[7]

More recently, thanks to the pioneering work of Costa's group,[8] another neutral subunit capable of establishing, like

[a] Dr. V. Amendola, Dr. G. Bergamaschi, Prof. L. Fabbrizzi, Dr. M. Milani
Dipartimento di Chimica Generale, Università di Pavia
via Taramelli 12, 27100 Pavia (Italy)
Fax: (+39) 0382-528544
E-mail: luigi.fabbrizzi@unipv.it

[b] Dr. M. Boiocchi
Centro Grandi Strumenti, Università di Pavia
via Bassi, 27100 Pavia (Italy)

Supporting information for this article is available on the WWW under http://dx.doi.org/10.1002/chem.200903190.

urea, a bifurcated hydrogen-bond interaction has been considered in the design of anion receptors: squaramide. Theoretical studies have shown the superiority of squaramide over urea as a hydrogen-bonding donor,[9] a feature that has been essentially ascribed to the increase of the aromatic character of the squaramide ring upon anion complexation.[10] A further contribution in the field involved the design of a macrotricyclic Cu^{II} cryptate that contained two squaramide moieties capable of including halide ions.[11] Recently, a squaramide-based chloride ion receptor, the anion binding cavity of which can be opened and closed by using carbonyl groups as valves, has been described.[12]

In this context, we intend to investigate in detail anion-recognition tendencies of the squaramide subunit, to be compared with those of the urea subunit. Anion binding of the urea derivative, equipped with the most powerful electron-withdrawing substituent (1,3-bis(4-nitrophenyl)-urea, **1**), towards anions in acetonitrile has been previously investigated by this group.[13] We report here the synthesis and the anion-binding properties of the squaramide analogue **2**, which has been investigated in MeCN through spectroscopic titration experiments. Moreover, the crystal structure of the hydrogen-bond complexes of **2** with chloride and bromide ions will be discussed. It is anticipated that, judging from the association constants with a variety of anions, squaramide is a better receptor than urea, with a special reference to halide ions. Such superiority can be accounted for by considering the structural features of the receptor–halide complexes.

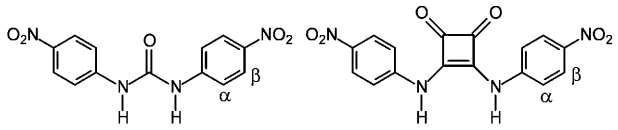

Results and Discussion

The crystal and molecular structures of the chloride and bromide complexes: The tendency of **2** to form 1:1 complexes with anions in the solid state was revealed by X-ray studies. In particular, on slow evaporation of a solution of equimolar amounts of **2** and $[BnEt_3N]Cl$ in MeCN, crystals of a salt of formula $[BnEt_3N][\mathbf{2}\cdots Cl]$ suitable for crystallographic studies were obtained. The ORTEP diagram of the complex is shown in Figure 1.

In particular, the crystal contains two asymmetrically equivalent $[\mathbf{2}\cdots Cl]^-$ hydrogen-bond complexes and the corresponding two $[BnEt_3N]^+$ counterions (not shown in Figure 1, but shown in Figure S7 of the Supporting Information). Each receptor establishes a bifurcated hydrogen-bond interaction with the chloride ion through the amide N–H fragments. Geometrical features of the N–H···Cl interactions

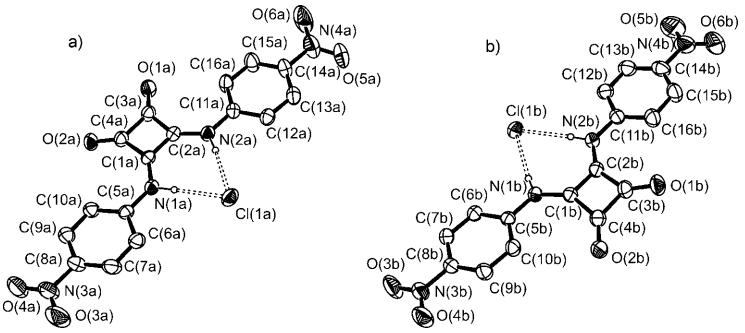

Figure 1. An ORTEP view of the two symmetrically independent molecules of the $[\mathbf{2}\cdots Cl]^-$ receptor–anion complex that constitute the crystal. (Thermal ellipsoids are drawn at the 30% probability level. Only hydrogen atoms involved in hydrogen bonds are shown. Hydrogen bonds have been drawn as dashed lines.) Atoms of the two non-equivalent receptor–anion complexes were named by adding a final "a" and "b" suffix to the same atom-naming scheme.

are reported in Table 1, together with those observed for the analogous $[\mathbf{2}\cdots Br]^-$ complex (vide infra). The donor–acceptor distances (N···Cl) fall in the range 3.10–3.14 Å, which corresponds to the formation of "moderate" hydrogen bonds, mainly electrostatic in nature, according to Jeffrey's classification.[14]

Table 1. Structural features of the hydrogen-bond interactions in $[\mathbf{2}\cdots Cl]^-$ and $[\mathbf{2}\cdots Br]^-$ receptor–anion complexes.

Donor group	D···A [Å]	H···A [Å]	D–H···A [°]	Acceptor atom
N(1a)–H(N1a)	3.10(1)	2.21(4)	177.3(31)	Cl(1a)
N(2a)–H(N2a)	3.13(1)	2.31(3)	170.4(32)	Cl(1a)
N(1b)–H(N1b)	3.14(1)	2.33(3)	172.5(32)	Cl(1b)
N(2b)–H(N2b)	3.14(1)	2.25(4)	174.3(30)	Cl(1b)
N(1)–H(N1)	3.31(1)	2.53(4)	169.5(31)	Br(1)
N(2)–H(N2)	3.27(1)	2.44(3)	173.7(32)	Br(1)

One of the two independent receptor moieties (**a**, with atom names reporting the "a" suffix) exhibits an almost coplanar molecular geometry: the deviations for C, N and O atoms that constitute the squaramide ring from their best plane are less than 0.01(1) Å, and the dihedral angles between the two phenyl rings and the squaramide unit are 0.2(1) and 3.4(1)°. The second receptor moiety, **b**, shows a slightly distorted squaramide unit, as the deviations of C, N and O atoms from the best plane fall in the range −0.11(1)–0.10(1) Å. Also, the dihedral angles between the two aromatic rings and the squaramide group (6.1(1) and 9.1(1)°) are appreciably greater than observed for the other complex.

Interestingly, the planarity of the moieties of the receptor allows the formation of face-to-face π-stacking interactions among all the phenyl rings of adjacent nitrophenyl arms. In particular, the crystal contains couples of centrosymmetrically related molecules formed by atoms carrying the "a" suffix, which are superimposed onto couples of centrosymmetrically related molecules, the atoms of which are labelled

with the "b" suffix. Each "a" and "b" centrosymmetrically related pair is characterised by two face-to-face π-stacked phenyl rings that show the same value of the centroid–centroid distance: 3.70(1) Å for the "a" molecular couple and 3.72(1) Å for the "b" molecular couple. Likewise, the two superimposed phenyl rings exhibit the same value for the closest C···C contact: 3.41(1) Å for the "a" molecular couple and 3.43(1) Å for the "b" molecular couple.

Analogous face-to-face π-stacking interactions are established between the phenyl rings of adjacent "a" and "b" receptor couples: the two centroid–centroid distances between the two adjacent phenyl rings are 3.61(1) and 3.94(1) Å, whereas the corresponding closest C···C contacts are 3.40(1) and 3.41(1) Å. These features favour the assembling of superimposed molecular receptors to form 1D molecular rows of face-to-face π-stacked molecules. The molecular rows extend along the *a* crystallographic axis of the crystal, as sketched in Figure 2.

The cyclobutene ring of any single receptor molecule points in the opposite direction with respect to the two closest receptors, thus preventing the formation of face-to-face π-stacking interactions between adjacent cyclobutene rings.

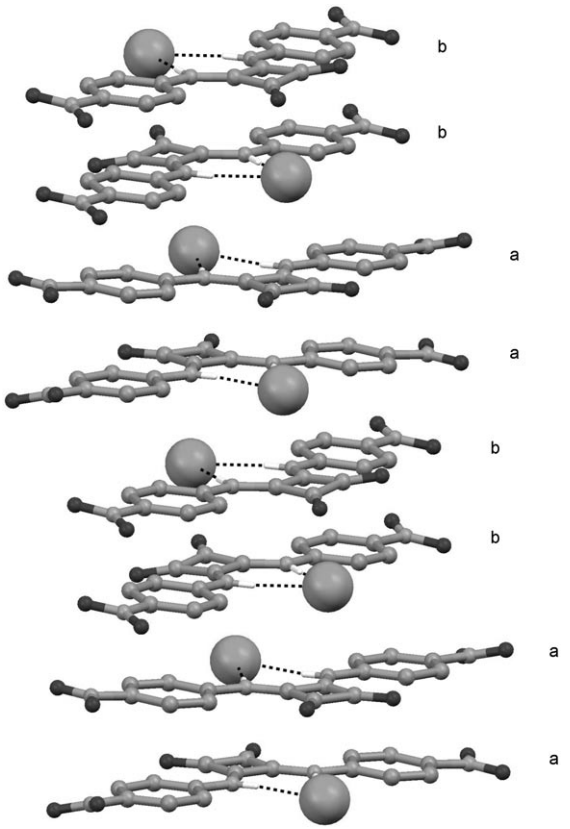

Figure 2. A simplified sketch of face-to-face π-stacked **2** receptor molecules that assemble to form infinite 1D molecular rows in the $[BnEt_3N]$-[**2**···Cl] crystal; the letters "a" and "b" identify the symmetrically equivalent molecules formed by atoms that carry the "a" or "b" suffix in the atom names. The Cl^- anions (large spheres) are bonded to receptors through hydrogen bonds (dashed lines) and are sandwiched between two cyclobutene rings, thereby establishing anion–π interactions.

However, each chloride ion ends up sandwiched between two cyclobutene rings of the two receptor molecules placed above and below any molecular receptor. Such a geometrical arrangement could favour the formation of anion–π interactions, as observed between anions and a variety of electron-poor six-membered aromatic rings.[15] In particular, in the present case, the anion–centroid distances are 3.62 and 3.64 Å for Cl(1a), and 3.46 and 3.67 Å for Cl(1b), respectively, whereas the shorter Cl···C contacts are: Cl(1a)···C(3b) 3.51(1), Cl(1a)···C(2a) 3.52(1), Cl(1b)···C(4b) 3.52(1) and Cl(1b)···C(1b) 3.54(1) Å. These distances are distinctly smaller than the sum of the van der Waals radii of the carbon atom, 1.70 Å,[16] and of the chloride ion, 2.47 Å,[17] that is, 4.17 Å, thereby indicating the occurrence of significant anion–π interactions. Recently, the crystal structure of the chloride complex of a squaramide derivative with an appended alkylammonium side chain has been reported.[18] In particular, the chloride ion establishes a definite π interaction with the cyclobutene-1,2-dione subunit, located over the ring plane at 3.55 Å.[18]

Crystals suitable for X-ray diffraction analyses were obtained also for the 1:1 complex with a bromide ion. The crystal and molecular structure of the $[Bu_4N]$[**2**···Br] complex salt, shown in Figure 3, indicates that receptor **2** establishes a bifurcated hydrogen-bonding interaction with the bromide ion, in the same way as observed for chloride. Donor–acceptor distances (Table 1) are appreciably larger than for the chloride ions, a behaviour that reflects the greater ionic radius of bromide.

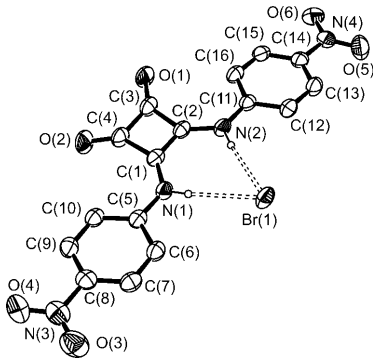

Figure 3. An ORTEP view of the $[$**2**···Br$]^-$ receptor–anion complex. (Thermal ellipsoids are drawn at the 30% probability level. Only hydrogen atoms involved in hydrogen bonds are shown. Hydrogen bonds have been drawn as dashed lines.) The tetrabutylammonium ion in not shown in this figure, but is shown in Figure S8 of the Supporting Information.

The $[Bu_4N]$[**2**···Br] complex salt also contains an almost coplanar **2** receptor: the mean deviation of C, N and O atoms that constitute the squaramide ring from their best plane is 0.03(1) Å, whereas the dihedral angles between the two phenyl rings and the squaramide unit are 6.6(1) and 9.2(1)°. As observed for the chloride analogue, in the crystal of the bromide complex two equivalent molecules of **2**, related to each other by an inversion centre, form couples

with extensive face-to-face π-stacking interactions among the phenyl rings of adjacent nitrophenyl arms. The centroid–centroid distance (3.65(1) Å), as well as the closest C···C contact for both adjacent phenyl rings (3.33(1) Å), are similar to those observed in the chloride complex. Moreover, in the present case, too, cyclobutene rings of adjacent molecules have opposite orientations and are excluded from face-to-face π-stacking interactions.

However, in contrast to what was observed for the chloride analogue, no extensive π-stacking interactions exist between adjacent couples in the crystal of the $[\mathbf{2}\cdots Br]^-$ complex, because only one of the two nitrophenyl groups ends up superimposed among adjacent molecular couples. The centroid–centroid distance between the superimposed phenyl rings of adjacent couples is 3.64(1) Å, whereas the closest C···C contact is 3.37(1) Å. These features favour the assembly of superimposed receptor couples according to a 1D zigzag-folded stacking, as illustrated in Figure 4.

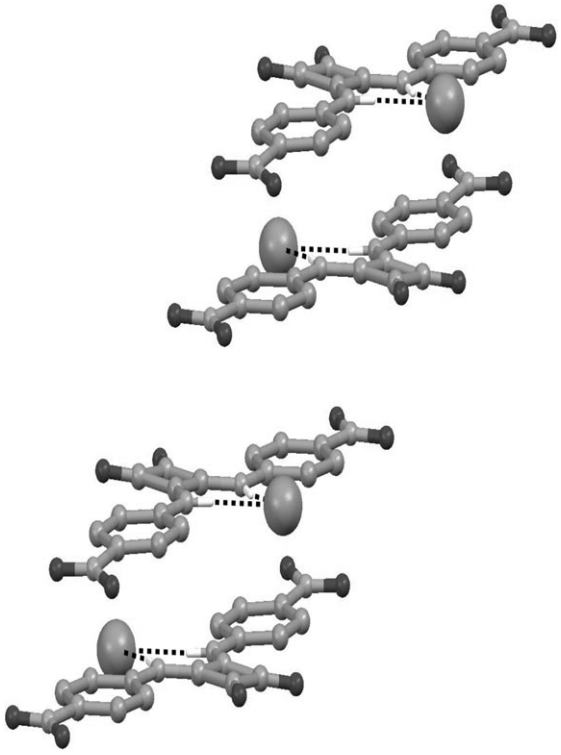

Figure 4. A simplified sketch of face-to-face π-stacked molecules of **2**, assembled to give a 1D zigzag-folded molecular chain in the crystal of the $[Bu_4N][\mathbf{2}\cdots Br]$ complex salt. Each bromide anion (large spheres) is bound to the receptor through hydrogen bonds (dashed lines) and is close to only one cyclobutene ring, placed according to a weak unidirectional anion–π interaction.

Notice that bromide ions are not sandwiched between two cyclobutene rings, but each Br^- ion is placed above one cyclobutene rings. The anion–centroid seems quite large (4.10(1) Å). In any case, the Br···C (Br(1)···C(3) 3.87(1) Å) contacts are shorter than the sum of the van der Waals radii of the carbon atom (1.70 Å)[16] and of the bromide ion (2.58 Å),[17] that is, 4.28 Å, thereby indicating the establishment of some anion–π interactions. It is therefore concluded that the overall stabilisation of the 3D packing in the crystal structure of both chloride and bromide complexes results from the dipolar character of both the nitrophenyl and squaramide rings, from the formation of π–π interactions between facing receptor molecules and, to some extent, from a π interaction between the anion and the cyclobutene subunit.

Moreover, it is worth noting here that receptor **2**, when interacting with chloride and bromide, exhibits an overall planar geometry. The planarity not only promotes the formation of face-to-face π-stacking interactions, but also favours the placement of the protons of the C_α–H fragments of the two phenyl substituents on positions suitable for the establishment of further C_α–H···$[X]^-$ interactions. In fact, the H_α protons lie on the plane defined by the bifurcated N–H···$[X]^-$ interaction. This favourable spatial arrangement plays a crucial role in determining the unusually high stability of halide complexes of **2** (vide infra).

The interaction of receptor 2 with anions in MeCN, studied by spectrophotometry: The interaction of receptor **2** with anions was investigated as a solution in MeCN through spectrophotometric titration experiments. In a typical experiment, a solution of **2** in MeCN was titrated with a standard solution of the tetraalkylammonium salt of the chosen anion. The occurrence of the receptor–anion interaction was documented by distinctive changes of the absorbance of the receptor in the UV/Vis region. Figure 5a and b show the spectrum of a solution of **2** in MeCN (solid line).

The spectrum displays two bands: one, centred at 272 nm (❶), ascribed to the highest-energy charge-transfer transition illustrated in Scheme 1, which results in the zwitterion with the negative charge being placed on one of the oxygen atoms of the carbonyl fragments and with the positive charge centred on one of the amide nitrogen atoms; the other, centred at 395 nm (❷) and corresponding to the lowest-energy transition, is responsible for the formation of the zwitterionic excited state in which the negative charge is located on one of the oxygen atoms of the nitro groups. Quite interestingly, semiempirical studies using the ZINDO/S method showed that moving from the HOMO to LUMO level induces a displacement of charge density on the nitro groups of the phenyl substituents, transition ❷; whereas, in the higher energy molecular orbital, the electron density in essentially localised over the squaramide subunit (transition ❶, see Figure S1 of the Supporting Information).

It is expected that the interaction of an anion at the amide N–H fragments stabilises both excited states, which retain a positive charge on one nitrogen atom, thus reducing the energy of the optical transition. This should induce a redshift of the two absorption bands. Indeed, upon anion addition, both charge-transfer bands undergo a definite redshift, as illustrated by representative examples in Figure 5, with chloride (a) and dihydrogenphosphate (b).

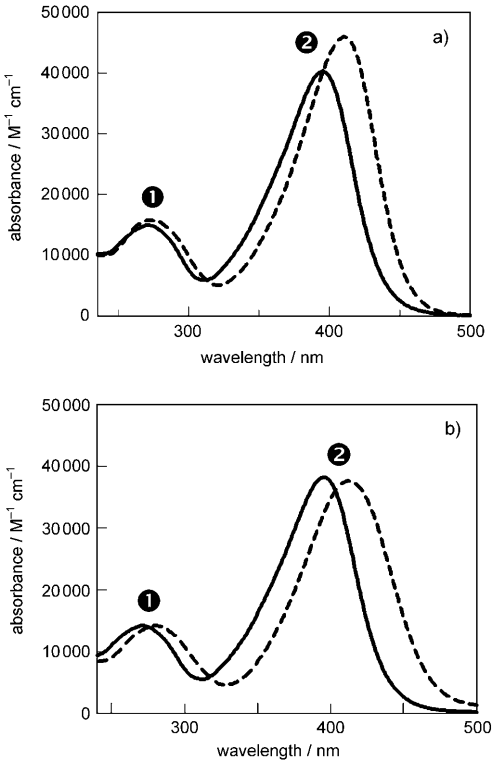

Figure 5. Solid lines: spectrum of a solution of receptor **2** in MeCN. Dashed lines: a) spectrum obtained after excess addition of $[Et_3Bn]Cl$; b) spectrum obtained after excess addition of $[Bu_4N]H_2PO_4$.

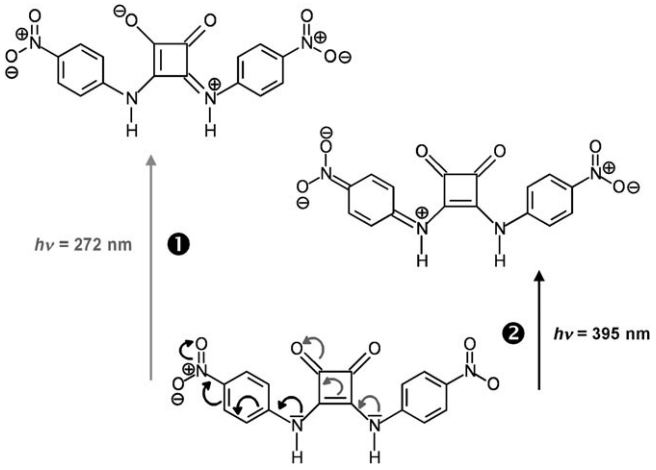

Scheme 1. The hypothesised charge-transfer transitions in receptor **2**.

The interaction of 2 with halides and oxoanions: Spectrophotometric titration experiments were carried out with halides and some selected oxoanions ($H_2PO_4^-$, NO_3^-, HSO_4^-, CH_3COO^-). The stoichiometry and the binding constants of the species present at the equilibrium were determined by treatment of spectrophotometric titration data by a non-linear least-squares procedure, using HyperQuad.[19] As an example, Figure 6a shows the family of spectra taken over

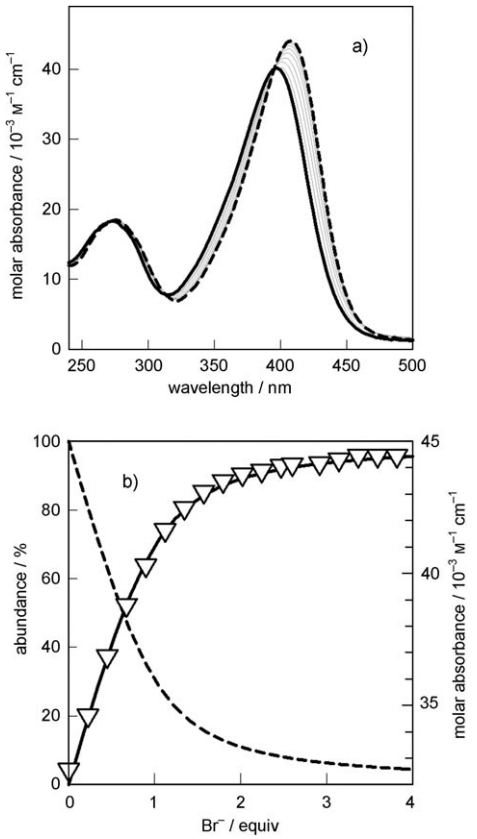

Figure 6. a) Family of spectra taken over the course of the titration of a 1×10^{-4} M solution of **2** (=LH) with a standard solution of $[Bu_4N]Br$ in MeCN. Dashed line: spectrum of receptor **2** prior to bromide addition. b) Lines: percent concentration of the species present at the equilibrium over the course of the titration with bromide (left axis). Triangles: absorbance at 410 nm, which monitors the formation of the $[LH\cdots Br]^-$ complex (right axis).

the course of the titration of a 1×10^{-4} M of **2** with a standard solution of $[Bu_4N]Br$, at 25 °C.

Upon bromide addition, the charge-transfer band of the receptor centred at 395 nm (ascribed to transition ❷) is significantly redshifted, whereas the displacement to higher wavelengths of the band centred at 272 nm (assigned to transition ❶) is much less pronounced. The presence of definite isosbestic points (at 310 and 392 nm) indicates that only two species coexist at the equilibrium. The profile of the molar absorbance at 410 nm versus equivalents of bromide (the triangles in Figure 6b) suggests the formation of a receptor/anion complex of 1:1 stoichiometry, the structure of which should be the same as that observed in the solid state and illustrated in Figure 3. Results can thus be interpreted on the basis of the following equilibrium [Eq. (1); LH = **2**, X = Br]:

$$LH + X^- \rightleftharpoons [LH\cdots X]^- \quad (1)$$

in which $[LH\cdots X]^-$ represents the receptor–anion hydrogen-bond complex. Through the non-linear least-squares treatment of the titration profiles over the 350–450 nm interval,

the association constant of Equation (1) (X = Br) was determined ($\log K = 4.70 \pm 0.01$). From the $\log K$ value, the percent concentration of the species present at the equilibrium (abundance) over the course of the titration could be calculated (lines in Figure 6b). It is observed that the absorbance of the band of the association complex superimposes well on the concentration profile of $[LH\cdots Br]^-$, thus corroborating the integrity of the model.

Analogous titration experiments were performed with other anions. In all cases, with the notable exception of F^- and CH_3COO^-, the formation of a receptor/anion complex of 1:1 stoichiometry was ascertained, even in the presence of a large anion excess. Pertinent $\log K$ values for equilibria of the type shown in Equation (1) are reported in Table 2.

The interaction of 2 with fluoride and acetate—the occurrence of N–H deprotonation: The more basic anions CH_3COO^- and F^- displayed a more complex behaviour. Figure 7a shows the family of spectra taken over the course of the titration of a 2×10^{-5} M solution of **2** (LH) with a 2×10^{-3} M solution of $[Bu_4N]F$.

It appears that the interaction of the fluoride ion with receptor **2** takes place according to two well-defined steps. In particular, upon addition of the first equivalent of F^-, a distinct redshift of the charge-transfer bands of the receptor is observed, which is ascribed to the formation of the hydrogen-bond complex $[LH\cdots F]^-$, according to Equation (2):

$$LH + F^- \rightleftharpoons [LH\cdots F]^- \quad (2)$$

The 1:1 stoichiometry of the complex is confirmed by the titration profile shown in Figure 7b. In particular, the absorbance at 427 nm (open triangles), pertinent to the band associated to the $[LH\cdots F]^-$ complex, increases up to the addition of 1 equiv of F^-, then abruptly decreases. It is anticipated that the absence of a smooth curvature in the profile precludes any safe determination of K_1, the constant for Equation (2). Then, upon addition of the second equivalent of F^-, the intensity of the band centred at 425 nm rapidly decreases, and a new band forms and develops at 500 nm. Appearance of a band at high wavelengths upon addition of excess

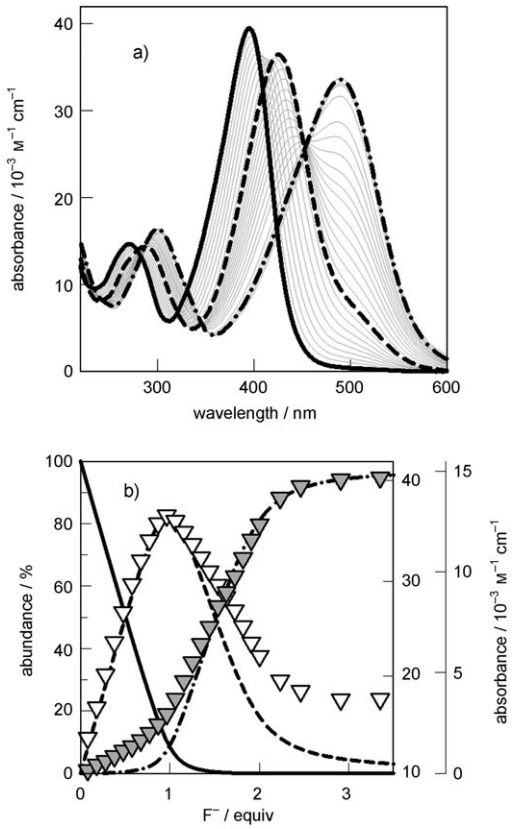

Figure 7. a) Family of spectra taken over the course of the titration of a 2×10^{-5} M solution of **2** (=LH) with a 2×10^{-3} M solution of $[Bu_4N]F$ in MeCN. b) Lines: percent concentration of the species present at the equilibrium over the course of the titration (left axis). Open triangles: absorbance at 427 nm, which monitors the formation of the $[LH\cdots F]^-$ complex (right axis). Grey triangles: absorbance at 540 nm, which monitors the formation of the deprotonated receptor L^- (far-right axis).

fluoride has been previously observed with urea[13] and thiourea derivatives[20] equipped with electron-withdrawing substituents, and it has been associated with the occurrence of an equilibrium of the following type [Eq. (3)]:

$$[LH\cdots F]^- + F^- \rightleftharpoons L^- + [HF_2]^- \quad (3)$$

Table 2. Constants of the complex formation equilibria that involve a solution of receptors **2** and **1** (=LH) in MeCN at 25 °C. The standard deviations are given in parentheses.

Anion: X^-	$\log K_1$ $LH + X^- \rightleftarrows [LH\cdots X]^-$		$\log K_2$ $[LH\cdots X]^- + X^- \rightleftarrows L^- + [HX_2]^-$		$\Delta\lambda$ [nm][a] (395 nm)	$\Delta\lambda$ [nm][a] (272 nm)
	2	**1**[b]	**2**	**1**[b]		
F^-	8.0(2)	7.4(1)	6.0(2)	6.4(1)	27	11
Cl^-	6.05(2)	4.55(1)	–	–	16	4
Br^-	4.70(1)	3.22(3)	–	–	13	2
I^-	3.51(2)	<2	–	–	6	0
NO_3^-	3.68(1)	3.65(5)	–	–	8	2
NO_2^-	4.75(2)	4.33(1)	–	–	13	4
HSO_4^-	4.02(3)	4.26(1)	–	–	9	3
$H_2PO_4^-$	5.42(7)	5.37(1)	–	–	26	6
CH_3COO^-	6.5(2)	6.61(1)	3.1(2)	–	23	10

[a] The variable $\Delta\lambda$ [nm] refers to the extent of the redshift of the pertinent charge-transfer absorption band after the addition of excess anion. [b] Values from ref. [13].

in which an N–H fragment of the receptor is deprotonated while the $[HF_2]^-$ hydrogen-bond self-complex forms. Thus, it is suggested that N–H deprotonation takes place also with the squaramide-based receptor **2**. In particular, the absorbance at 540 nm has been considered to monitor the deprotonation process of the receptor (grey triangles in Figure 8b): it is observed that a limiting value of absorbance is achieved upon addition of 4 equiv or more of F^-. It has been mentioned that K_1 has too high a value for being determined through a least-squares curve-fitting procedure (e.g., using the HyperQuad package).[19] However, we could obtain approximate values of K_1 and K_2 by doing tentative fitting of the two titration profiles shown in Figure 7b. In particular, several couples of K_1 and K_2 were chosen, and pertinent percent concentration curves of the species present at the equilibrium were calculated and were 'visually' fitted on the titration profiles. The best superimposition of lines (concentration) on symbols (absorbance) was obtained by assuming $\log K_1 = 8.0 \pm 0.2$ and $\log K_2 = 6.0 \pm 0.2$. Uncertainties were estimated by considering that a variation of 0.2 log units of $\log K$ values caused a visually detectable deviation from best fitting. It has to be noted that concentration curves may substantially deviate from titration profiles over the course of the titration, for instance, the concentration of the $[LH\cdots F]^-$ complex (dashed line) from the titration profile at 427 nm (open triangles) after the addition of 2 equiv of F^- (see Figure 7b). Deviations have to be ascribed to the fact that chosen absorbances do not pertain to a single species but rather result from the contribution of the different species present at equilibrium, sometimes in comparable amounts.

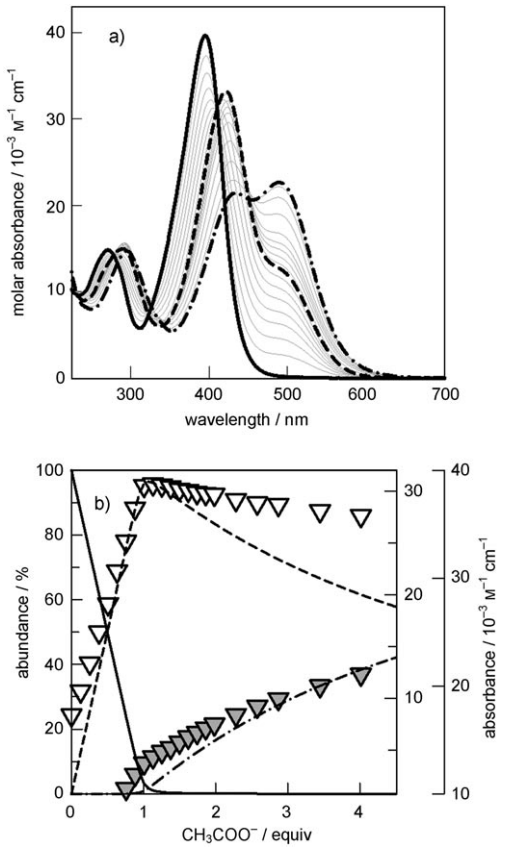

Figure 8. a) Family of spectra taken over the course of the titration of a 2×10^{-4} M solution of **2** (=LH) with a standard solution of $[Bu_4N]CH_3COO$ in MeCN. Solid line: spectrum of receptor **2** prior to addition of acetate. Short dashed line: spectrum taken after the addition of 1 anion equivalent. Dash-dot line: spectrum taken after the addition of four equivalents. b) Lines: percent concentration (abundance) of the species present at the equilibrium over the course of the titration with acetate (left axis). Solid line: uncomplexed receptor **2** (L). Short-dashed line: hydrogen-bond complex $[LH\cdots CH_3COO]^-$. Long-dashed line: deprotonated receptor L^-. Open symbols: absorbance at 435 nm, which monitors the formation of the $[LH\cdots CH_3COO]^-$ complex (right axis). Filled symbols: absorbance at 500 nm, which monitors the formation of the deprotonated form of the receptor, L^- (far-right axis).

It had been observed with the analogous urea-based receptor **1** that N–H deprotonation occurred only on titration with F^-, a circumstance attributed to the especially high stability of the hydrogen-bond self-complex $[HF_2]^-$. Other basic X^- anions, including CH_3COO^-, formed only the $[LH\cdots X]^-$ complex, even in the presence of a large excess of X^-.

Figure 8a shows the family of spectra taken over the course of the titration of a 2×10^{-4} M solution of **2** with a standard solution of $[Bu_4N]CH_3COO$ in MeCN. It is observed that, upon addition of the first equivalent of acetate, the amide-to-nitrophenyl charge-transfer band undergoes the typical redshift that corresponds to the formation of the 1:1 hydrogen-bonding complex. However, upon further anion addition, the band associated with the hydrogen-bond complex, centred at 435 nm, decreases in intensity, and a new band develops at 500 nm. The appearance of this band clearly indicates the occurrence of the N–H deprotonation, according to an equilibrium of the type shown in Equation (3). In particular, the formation of a $[CH_3COOH\cdots CH_3COO]^-$ hydrogen-bond self-complex has to be hypothesised. Indeed, the $[CH_3COOH\cdots CH_3COO]^-$ species has been previously isolated as a solid and its structure had been elucidated through a neutron-diffraction experiment.[21] A sketch based on deposited crystallographic coordinates is shown in Figure 9.

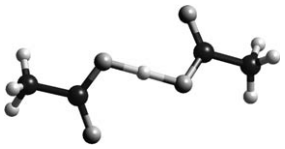

Figure 9. The molecular structure of the $[CH_3COOH\cdots CH_3COO]^-$ hydrogen-bond self-complex; the sodium counterion has been omitted for clarity. A proton is shared by the oxygen atoms of two equivalent acetate subunits, as inferred from neutron diffraction studies.[21] Structure redrawn from data deposited at the Cambridge Crystallographic Data Centre.

In the present case, too, the titration profile based on absorbances pertinent to the $[LH\cdots CH_3COO]^-$ complex (dashed line) does not show a smooth curvature. Thus, $\log K$ values were tentatively determined through visual fitting of abundance curves and titration profiles, as shown in Fig-

ure 9b: $\log K_1 = 6.5 \pm 0.2$; $\log K_2 = 3.2 \pm 0.2$. Notice that the $\log K_2$ value is approximately three orders of magnitude lower than that observed for the corresponding reaction with fluoride. This may reflect the lower stability of the $[CH_3COOH\cdots CH_3COO]^-$ self-complex with respect to $[HF_2]^-$. In fact, even upon excess addition of CH_3COO^- (4 equiv), only 40% of the deprotonated receptor L^- has been spectrophotometrically detected.

Figure 10 shows the ^{1}H NMR spectra taken over the course of the titration with acetate of a 5×10^{-3} M solution of **2** in [D$_6$]DMSO. DMSO was chosen as a solvent to afford a concentration suitable for ^{1}H NMR spectroscopic studies (5×10^{-3} M). It is observed that H_α and H_β protons undergo an upfield shift upon addition of acetate. Upfield shift of both H_α and H_β protons of the nitrophenyl substituents had been observed in the titration of **1** with fluoride, thereby indicating deprotonation of one of the urea N–H fragments.[13]

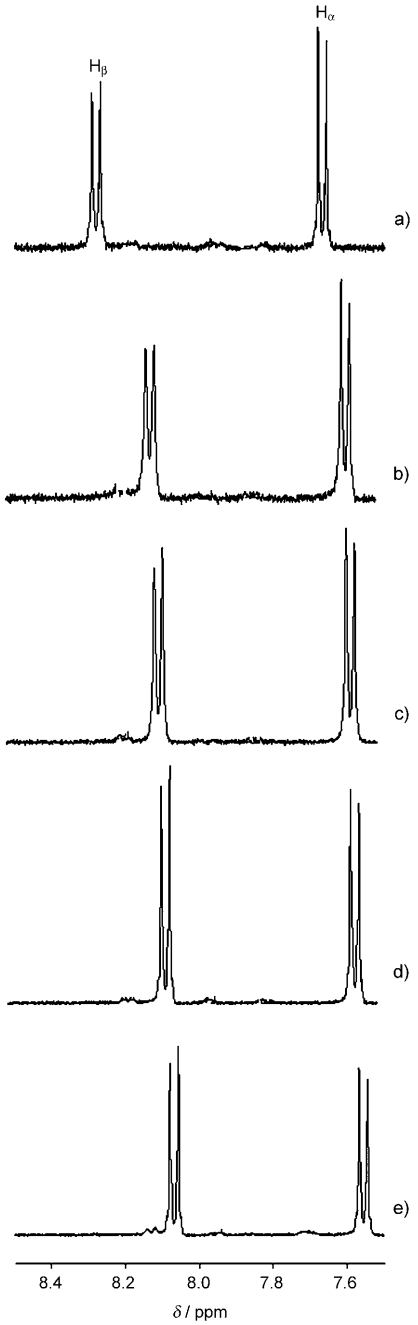

Figure 10. ^{1}H NMR spectra taken over the course of the titration of a 5×10^{-3} M solution of **2** in [D$_6$]DMSO with a standard solution of acetate. The spectra are taken in the absence of a) anion and after the addition of b) 0.25, c) 0.5, d) 0.75 and e) 1.25 equiv of acetate.

The fact that the upfield shift is observed also upon addition of 0.25 equiv of CH_3COO^- may indicate that in the present experiment deprotonation of the receptor begins to occur well before one equivalent. This may be due 1) to the distinctly polar nature of the used solvent (DMSO), which favours the formation of charged species and the occurrence of the acid–base neutralisation process, and 2) to the fact that titration has been carried out at a concentration 25-fold higher than the spectrophotometric one. It has to be noted that upfield shift results from a through-bond mechanism, which brings electron density to the phenyl substituents and causes a shielding effect. Upon addition of the first aliquots of acetate, such an upfield shift is significant for the C–H_β signal and moderate for the C–H_α signal. In fact, in the $[LH\cdots CH_3COO]^-$ complex, the C–H_α fragment is polarised by the close anion, thus inducing a deshielding effect, which partially reduces the upfield shift originated by the through-bond mechanism.

Looking at correlations between thermodynamic and spectral data: The $\log K$ values are related to the free-energy change, $\Delta G°$, which in turn results from the combination of two distinct contributions: 1) the enthalpy term, $\Delta H°$, which comprises all binding energies, including receptor–anion hydrogen-bond interactions, and 2) the entropy term, $T\Delta S°$, which mainly refers to changes in the solvation of reagents and products and to solvent reorganisation during the complexation process.[22] However, in the absence of calorimetric data, it is assumed that in a homogeneous class of anions the entropy change does not vary too much, so that the trends of $\log K$ values are interpreted in terms of bonding energy. In this sense, anion recognition is currently being accounted for on a molecular basis. On the other hand, spectral data may give direct information about the intensity of bonding interactions within the complex. In particular, the redshift ($\Delta\lambda$ in nm) of the charge-transfer bands is related to the energy of the interaction between the anion and the receptor in its excited state.

Figure 11a discloses the existence of a reasonable linear correlation between $\log K$ and the redshift of the band at 395 nm, which refers to the charge-transfer transition ❷ in Scheme 1, and holds for both halides and oxoanions. Figure 11b pertains to the band at 272 nm (transition ❶ in Scheme 1). Although a general increase in $\log K$ with $\Delta\lambda$ is observed, it appears that halides and oxoanions display distinctly different behaviours, since corresponding points lie on two different, nearly parallel straight lines. In particular, halides seem to be able to induce the formation of negative charge onto squaramide carbonyl oxygen atoms to a greater extent than oxoanions. The origin of this effect is not clear.

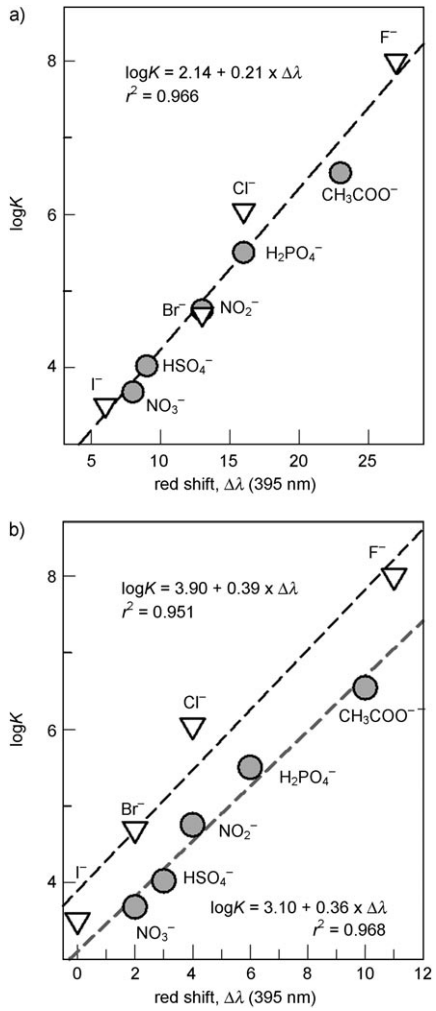

Figure 11. a) Plot of $\log K$ versus the redshift of the band of receptor **2** centred at 395 nm (charge-transfer transition ❷ in Scheme 1); b) plot of $\log K$ versus the redshift of the band of receptor **2** centred at 272 nm (charge-transfer transition ❶ in Scheme 1).

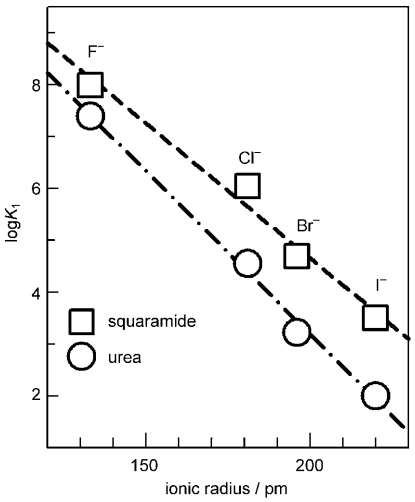

Figure 12. Plot of $\log K_1$ versus halide ionic radius, which illustrates the electrostatic nature of the receptor–halide interaction within the hydrogen-bond complex $[LH\cdots X]^-$.

However, it may be in some way related to the relatively higher stability of halide complexes of **2** with respect to those of oxoanions, as compared to corresponding ones of the urea-based receptor **1** (vide infra).

A comparison of the anion-binding tendencies of squaramide- and urea-based receptors: The $\log K$ values for the anion-binding equilibria of **2** are compared in Table 2 to those of the analogous urea-based receptor **1**.[13] It is observed that 1) for both receptors, halide complex stability decreases along the series $F^- > Cl^- > Br^- > I^-$, but for a given anion, **2** forms a complex 1 to 2 orders of magnitude more stable than **1**; 2) in the case of oxoanions, both receptors form with a given anion complexes of the same stability, which decreases according to the sequence $CH_3COO^- > H_2PO_4^- > NO_2^- > HSO_4^- > NO_3^-$.

As far as the interaction with halide ions is concerned, Figure 12 reveals the existence of a linear correlation between $\log K_1$ values and anion radius. Such a relationship holds for both receptors **1** and **2** and points towards a predominantly electrostatic nature of the receptor–halide interaction (the higher the charge density—electric charge over ionic radius—of the anion, the stronger the interaction established). In particular, the squaramide derivative **2** seems capable of more-intense electrostatic interactions with halides than the urea derivative **1**. Such different behaviour can be accounted for through an inspection of available structural data.

Figure 13a displays the molecular structure of the $[LH\cdots Cl]^-$ complex (LH = **2**), the ORTEP view of which is shown in Figure 3, whereas Figure 13b shows the structure of the chloride complex of the urea derivative *N*,*N*′-di-4-chlorophenylurea (**3**),[23] the only chloride complex of a diarylurea-based receptor for which structural data are available. In Table 3, distances relevant to the hydrogen-bond in-

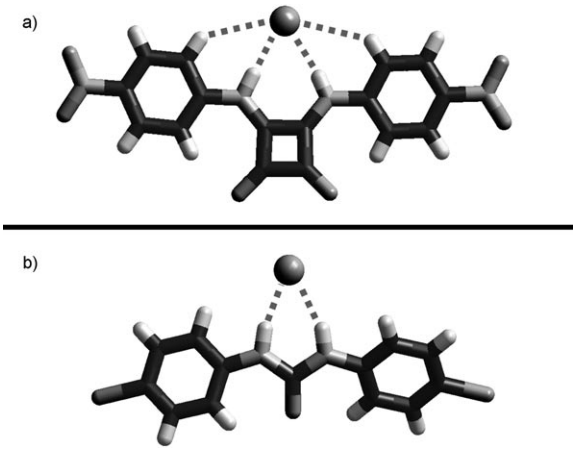

Figure 13. Structures of the $[LH\cdots Cl]^-$ complexes with squaramide- and urea-based receptors; a) LH = **2**, this work; b) LH = **3**.[23] Structure redrawn from data deposited at the Cambridge Crystallographic Data Centre.

Table 3. N–H and C_α–H contact distances for bifurcated interactions in $[L–H\cdots Cl]^-$ complexes with squaramide- and urea-based receptors.

Receptor	N–H···Cl [Å]	N—Cl [Å]	C_α–H···Cl [Å][a]	C_α···Cl [Å][b]	Ref.
2	2.21, 2.33	3.10, 3.14	3.06, 3.14	3.78, 3.86	this work
3	2.24, 2.40	3.14, 3.33	3.34, 4.15	4.03, 4.64	[23]

[a] Average value from 288 observed distances is (3.07 ± 0.15) Å.[24] [b] Average value from 288 observed distances is (3.82 ± 0.15) Å.[24]

teractions are given. It can be seen that, as far as interactions of Cl^- with N–H fragments are concerned, H···Cl and N···Cl distances exhibit comparable values, which indicate a similar contribution to the binding energy and to the magnitude of $\log K$ values.

However, significant differences are observed in the contact distances between chloride and the C_α–H fragments of the phenyl substituents. The occurrence of hydrogen-bond interactions between anions and aromatic C–H groups has been observed in a large variety of examples and it has been critically reviewed in a recent paper.[24] It is observed that in the squaramide complex C_α–H···Cl and C_α···Cl distances fall in the range expected for the establishment of a definite interaction (see values in Table 3). On the other hand, in the case of the urea-based receptor **3**, pertinent distances are distinctly beyond the range of interaction. Thus, the extra energy observed in the interaction with chloride of **2** with respect to **1** ($\Delta\log K = 1.5$, $\Delta\Delta G° = -8.6\ kJ\,mol^{-1}$) seems to be ascribed to the contribution of the additional hydrogen-bond bifurcated interaction with the two aryl C_α–H fragments. This should depend upon the higher convergence of these fragments, which are therefore placed closer and better oriented with respect to the anion.

The different nature of the interaction of the Cl^- ion with receptors **1** and **2** has been documented also by ^1H NMR spectroscopic studies. Figure 14a shows the spectra taken for a 5×10^{-3} M solution in **1** in [D_6]DMSO, in the absence and in the presence of a fourfold excess of chloride. Anion addition induces a downfield shift of $\delta = 1.32$ ppm of the N–H signal, thereby indicating the establishment of a hydrogen-bond interaction. On the other hand, a fivefold excess addition of chloride to a 5×10^{-3} M solution of **2** in [D_6]DMSO (see spectra in Figure 14b) induces: 1) a downfield shift of the N–H signal ($\delta = 1.35$ ppm), thereby indicating a hydrogen-bonding interaction of comparable intensity with respect to urea derivative **1**, and 2) a highly detectable downfield shift of the C_α–H signal, whereas the C_β–H signal does not experience any measurable shift. This indicates the existence of a definite hydrogen-bond interaction between the two C_α–H groups and the chloride ion. Such an interaction is not established with receptor **1**, as demonstrated by the insensitivity of the C_α–H signal to anion addition (see Figure 14a).

This additional hydrogen-bond contribution from C_α–H fragments seems to be present also in the bromide complex. In fact, in the solid complex, C_α–H···Br distances are 3.11 and 3.18 Å (to be compared with the average value of (3.19 ± 0.17) Å, based on 180 observed distances),[24] whereas C_α···Br distances are 3.87 and 3.93 Å (to be compared with the average value of (3.94 ± 0.16) Å).[24]

Quite surprisingly, such an additional contribution from convergent C_α–H fragments does not seem to operate in the case of oxoanions, which form complexes of similar stability with both **1** and **2**. This may suggest that the interactions of the N–H fragments of **1** and **2**, whether with halides or with oxoanions, have a different nature. Indeed, each N–H fragment of ureas and squaramides establishes an individual hydrogen-bond interaction with an oxygen atom of the oxoanion, according to a parallel mode, as sketched in Scheme 2.

In particular, it has been pointed out that hydrogen bonding should be considered as a 'frozen' proton transfer from the hydrogen-bond donor atom to the hydrogen-bond ac-

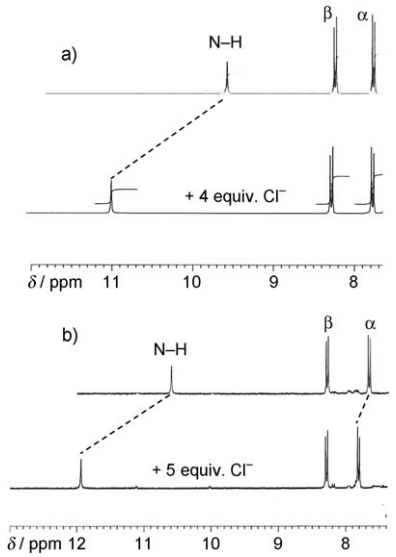

Figure 14. a) ^1H NMR spectra taken over the course of the titration of a 5×10^{-3} M solution of **1** in [D_6]DMSO in the absence and in the presence of a fourfold excess of chloride; b) ^1H NMR spectra taken over the course of the titration of a 5×10^{-3} M solution of **2** in [D_6]DMSO in the absence and in the presence of a fivefold excess of chloride.

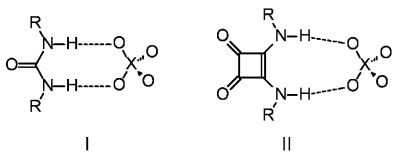

Scheme 2. The hydrogen-bond interaction with oxoanions of urea-based (I) and squaramide-based (II) receptors. Urea forms an eight-membered chelate ring with the oxoanion, squaramide a nine-membered one. The formation of the latter geometrical arrangement has been observed (through X-ray diffraction studies) in the nitrate complex of the squaramide-based receptor 4-bis[2-(2-pyridyl)ethylamino]-3-cyclobutene-1,2-dione.[25]

ceptor atom;[26] in the present case, this is from the amide nitrogen atom to the oxygen atom of the oxoanion. The more acidic the donor and the more basic the acceptor, the more advanced the proton transfer. From this perspective, it would seem that the two hydrogen-bond donors **1** and **2** give rise with a chosen oxoanion to proton-transfer processes at the same state of advancement. This would imply that the polarisation of the N–H fragments is essentially dictated by the nitrophenyl electron-withdrawing substituents, whereas the carbonyl group(s) play a minor role. Such a hypothesis might contrast with the observation that **2** is deprotonated in the presence of CH_3COO^-, and **1** is not. However, it must be considered that deprotonation of **2** is favoured by the great stabilisation experienced by the L^- ion, due to the negative charge delocalisation extended to the entire molecular framework and that may involve two carbonyl groups, as illustrated by the resonance formulae in Scheme 3. This term is less favourable for **1** in view of 1) the smaller molecular framework and 2) the presence of a single C=O group.

In any case, the sequence of $\log K_1$ values ($CH_3COO^- > H_2PO_4^- > NO_2^- > HSO_4^- > NO_3^-$) parallels the intrinsic basicity of oxoanions, thus confirming the acid–base nature of the receptor–anion interaction.

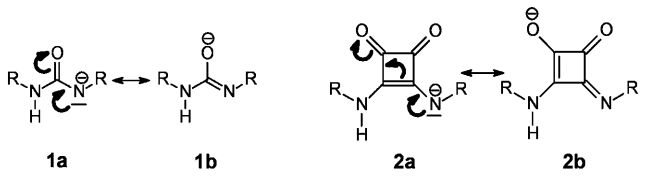

Scheme 3. Resonance formulae of the deprotonated forms of a urea-based (**1a** and **1b**) and of a squaramide-based (**2a** and **2b**) receptor.

Conclusion

Urea is currently being employed as a versatile subunit in the synthesis of anion receptors of increasing complexity.[5] Theoretical efforts have been made for the computer-aided design of neutral receptors that contain urea moieties for targeting anions of varying geometrical features.[6] This work has demonstrated that the squaramide subunit can rightfully challenge urea as a building block in the synthesis of neutral receptors for anions. In fact, if it establishes with oxoanions hydrogen-bonding interactions of an energy comparable to those observed with urea derivatives, with halides it gives complexes of definitely higher stability, thanks to the presence of convergent aryl C_α–H fragments that act as additional hydrogen-bond donors. In conclusion, squaramide-based receptors are expected to donate four hydrogen bonds to monoatomic anions such as halides, which makes them superior to their urea-based counterparts, which are capable of donating only two hydrogen bonds. Chemical stability of the squaramide framework and ready availability of intermediates provide additional benefits, which may encourage synthetic chemists toward the design of neutral multisite receptors based on the squaramide subunit.

Experimental Section

General procedures and materials: All reagents for syntheses were purchased form Aldrich/Fluka and used without further purification. Mass spectra were acquired using a Thermo-Finnigan ion trap LCQ Advantage Max instrument equipped with an ESI source. ^{1}H NMR spectra were taken using a Bruker ADVANCE 400.

Instruments: UV/Vis spectra were run using a Varian Cary 100 SCAN spectrophotometer. All titrations were performed at (25.0±0.1) °C. Titration data were processed with the Hyperquad package[19] to determine the equilibrium constants (reported in Table 2). Abundance profiles of the species at the equilibrium were drawn by using the program HySS.[27]

Synthesis of 2: Squaric acid chloride (0.15 g) was added to a suspension of 1-amino-4-nitrobenzene (0.41 g) in toluene. The mixture was heated at reflux for 24 h; the obtained red precipitate was filtered, washed with methanol and dried under vacuum. After recrystallisation, a pure product was obtained (0.21 g, 60%). ^{1}H NMR ([D$_6$]DMSO): δ=10.7 (s, 2H), 8.3 (d, 2H), 8.2 (d, 2H), 7.95 (s, 1H), 7.85 (d, 2H), 7.7 ppm (d, 2H); MS (ESI; MeOH): m/z: 353 $[M-1]^-$, 354 $[M+1]^+$, 399 $[M+HCOOH]^+$.

X-ray crystallographic studies: Diffraction data for a yellow crystal (dimensions of about 0.50×0.43×0.32 mm) of the [Bu_4N][**2**···Br] molecular complex were collected at ambient temperature by means of an Enraf–Nonius CAD4 four-circle diffractometer equipped with a punctual detector (scintillation counter). The [$BnEt_3N$][**2**···Cl] complex salt forms only small single crystals and diffraction data for an orange crystal (dimensions of about 0.08×0.06×0.04 mm) have been collected by means of a Bruker-Axs CCD-based diffractometer. Both diffractometers work with graphite-monochromatised $Mo_{K\alpha}$ X-radiation (λ=0.71073 Å). Crystal data for the two molecular complexes are shown in Table 4.

Data reductions (including intensity integration, background, Lorentz and polarisation corrections) for intensities collected using the conventional diffractometer were performed with the WinGX package;[28] absorption effects were evaluated with the psi-scan method,[29] and absorption correction was applied to the data (min/max transmission factors were 0.592/0.673). Frames collected using the CCD-based diffractometer were processed with the SAINT software,[30] and intensities were corrected for Lorentz and polarisation effects; absorption effects were empiri-

Table 4. Crystal data for the investigated complex salts.

	[Bu_4N][**2**···Br]	[$BnEt_3N$][**2**···Cl]
formula	$C_{32}H_{46}Br\,N_5O_6$	$C_{58}H_{64}Cl_2N_{10}O_{12}$
M_r	676.64	1164.10
crystal system	triclinic	triclinic
space group	$P\bar{1}$ (no. 2)	$P\bar{1}$ (no. 2)
a [Å]	12.033(5)	14.225(1)
b [Å]	12.118(2)	14.734(1)
c [Å]	13.697(3)	15.865(1)
α [°]	87.04(2)	86.84(1)
β [°]	64.29(2)	64.44(1)
γ [°]	76.20(2)	74.89(1)
V [Å^3]	1744.5(9)	2889.6(3)
Z	2	2
ρ_{calcd} [g cm^{-3}]	1.288	1.338
μ ($Mo_{K\alpha}$) [mm^{-1}]	1.226	0.183
scan type	ω scans	ω scans
θ range [°]	2–28	2–25
measured reflns	8841	31276
unique reflns	8362	10238
R_{int}	0.040	0.049
strong data ($I>2\sigma(I)$)	3613	5944
refined parameters	403	751
$R1$, $wR2$ (strong data)	0.0562, 0.1685	0.0612, 0.1130
$R1$, $wR2$ (all data)	0.1048, 0.1370	0.1597, 0.1934
GOF	1.004	1.021
max/min residuals [e Å^{-3}]	0.34/−0.38	0.30/−0.25

cally evaluated by the SADABS software,[31] and absorption correction was applied to the data (min/max transmission factors were 0.891/0.992). Both crystal structures were solved by direct methods (SIR 97)[32] and refined by full-matrix least-squares procedures on F^2 using all reflections (SHELXL 97).[33] Anisotropic displacement parameters were refined for all non-hydrogen atoms. Hydrogen atoms bonded to C atoms were placed at calculated positions with the appropriate AFIX instructions and refined using a riding model; hydrogen atoms bonded to N atoms and defining the N−H···[halogen] interactions were located in the final ΔF maps; their positions were successively refined during the final least-squares procedures without restraints on the atom coordinates.

CCDC-754724 ([Bu_4N][**2**···Br]) and 754725 ([$BnEt_3N$][**2**···Cl) contain the supplementary crystallographic data for this paper. These data can be obtained free of charge from The Cambridge Crystallographic Data Centre via www.ccdc.cam.ac.uk/data_request/cif.

Acknowledgements

The financial support of the Italian Ministry of University and Research and of the University of Pavia is gratefully acknowledged.

[1] C. Caltagirone, P. A. Gale, *Chem. Soc. Rev.* **2009**, *38*, 520–563; V. Amendola, L. Fabbrizzi, *Chem. Commun.* **2009**, 513–531; P. A. Gale, S. E. García-Garrido, J. Garric, *Chem. Soc. Rev.* **2008**, *37*, 151–190; J. L. Sessler, P. A. Gale, W.-S. Cho, *Anion Receptor Chemistry*, RSC, Cambridge, **2006**; V. Amendola, D. Esteban-Gómez, L. Fabbrizzi, M. Licchelli, *Acc. Chem. Res.* **2006**; *39*, 343–353; P. A. Gale, *Acc. Chem. Res.* **2006**, *39*, 465–475; J. W. Steed, *Chem. Commun.* **2006**, 2637–2649; F. P. Schmidtchen, *Coord. Chem. Rev.* **2006**, *250*, 2918–2928; V. Amendola, M. Bonizzoni, D. Esteban-Gómez, L. Fabbrizzi, M. Licchelli, F. Sancenón, A. Taglietti, *Coord. Chem. Rev.* **2006**, *250*, 1451–1470; A. P. Davis, *Coord. Chem. Rev.* **2006**, *250*, 2939–2951; K. Bowman-James, *Acc. Chem. Res.* **2005**, *38*, 671–678; R. Martínez-Máñez, F. Sancenón, *Chem. Rev.* **2003**, *103*, 4419–4476; P. D. Beer, E. J. Hayes, *Coord. Chem. Rev.* **2003**, *240*, 167–189; L. Fabbrizzi, M. Licchelli, A. Taglietti, *Dalton Trans.* **2003**, 3471–3479; P. D. Beer, P. A. Gale, *Angew. Chem.* **2001**, *113*, 502–532; *Angew. Chem. Int. Ed.* **2001**, *40*, 486–516.

[2] K. Choi, A. D. Hamilton, *J. Am. Chem. Soc.* **2003**, *125*, 10241–10249; S. O. Kang, J. M. Llinares, D. Powell, D. VanderVelde, K. Bowman-James, *J. Am. Chem. Soc.* **2003**, *125*, 10152–10153; S. Otto, S. Kubik, *J. Am. Chem. Soc.* **2003**, *125*, 7804–7805; C. R. Bondy, S. J. Loeb, *Coord. Chem. Rev.* **2003**, *240*, 77–99.

[3] P. A. Gale in *Encyclopedia of Supramolecular Chemistry* (Eds.: J. L. Atwood, J. W. Steed), Marcel Dekker, New York, **2004**, pp. 31–41; S. Nishizawa, P. Bühlmann, M. Iwao, Y. Umezawa, *Tetrahedron Lett.* **1995**, *36*, 6483–6486; S. Nishizawa, R. Kato, T. Hayashita, N. Teramae, *Anal. Sci.* **1998**, *14*, 595–597; K. P. Xiao, P. Bühlmann, Y. Umezawa, *Anal. Chem.* **1999**, *71*, 1183–1187; J. L. Jimenéz Blanco, J. M. Benito, C. O. Mellet, J. M. G. Fernández, *Org. Lett.* **1999**, *1*, 1217–1220; T. Hayashita, T. Onodera, R. Kato, S. Nishizawa, N. Teramae, *Chem. Commun.* **2000**, 755–756; T. Tozawa, Y. Misawa, S. Tokita, Y. Kubo, *Tetrahedron Lett.* **2000**, *41*, 5219–5223; R. Kato, S. Nishizawa, T. Hayashita, N. Teramae, *Tetrahedron Lett.* **2001**, *42*, 5053–5056; T. Gunnlaugsson, A. P. Davis, M. Glynn, *Chem. Commun.* **2001**, 2556–2557; S. Sasaki, D. Citterio, S. Ozawa, K. Suzuki, *J. Chem. Soc. Perkin Trans. 2* **2001**, 2309–2313; D. H. Lee, H. Y. Lee, K. H. Lee, J. L. Hong, *Chem. Commun.* **2001**, 1188–1189; G. Hennrich, H. Sonnenschein, U. Resch-Genger, *Tetrahedron Lett.* **2001**, *42*, 2805–2808; D. Jiménez, R. Martínez-Máñez, F. Sancenón, J. Soto, *Tetrahedron Lett.* **2002**, *43*, 2823–2825; D. H. Lee, H. Y. Lee, J.-I. Hong, *Tetrahedron Lett.* **2002**, *43*, 7273–7276; S. Kondo, M. Nagamine, Y. Yano, *Tetrahedron Lett.* **2003**, *44*, 8801–8804; T. Gunnlaugsson, P. E. Kruger, T. C. Lee, R. Parkesh, F. M. Pfeffer, G. M. Hussey, *Tetrahedron Lett.* **2003**, *44*, 6575–6578; F. Sansone, E. Chierici, A. Casnati, R. Ungaro, *Org. Biomol. Chem.* **2003**, *1*, 1802–1809; T. Gunnlaugsson, A. P. Davis, G. M. Hussey, J. Tierney, M. Glynn, *Org. Biomol. Chem.* **2004**, *2*, 1856–1863; V. Amendola, M. Boiocchi, D. Esteban-Gómez, L. Fabbrizzi, E. Monzani, *Org. Biomol. Chem.* **2005**, *3*, 2632–2639; A. L. Sisson, J. P. Clare, A. P. Davis, *Chem. Commun.* **2005**, 5263–5265; D. R. Turner, M. J. Paterson, J. W. Steed, *J. Org. Chem.* **2006**, *71*, 1598–1608; V. Amendola, M. Boiocchi, B. Colasson, L. Fabbrizzi, *Inorg. Chem.* **2006**, *45*, 6138–6147; M. Allevi, M. Bonizzoni, L. Fabbrizzi, *Chem. Eur. J.* **2007**, *13*, 3787–3795; L. Pescatori, A. Arduini, A. Pochini, F. Ugozzoli, A. Secchi, *Eur. J. Org. Chem.* **2008**, 109–120; C. Caltagirone, J. R. Hiscock, M. B. Hursthouse, M. E. Light, P. A. Gale, *Chem. Eur. J.* **2008**, *14*, 10236–10243; D. Meshcheryakov, F. Arnaud- Neu, V. Bohmer, M. Bolte, J. Cavaleri, V. Hubscher-Bruder, I. Thondorf, S. Werner, *Org. Biomol. Chem.* **2008**, *6*, 3244–3255.

[4] P. Anzenbacher, Jr., R. Nishiyabu, M. A. Palacios, *Coord. Chem. Rev.* **2006**, 2929–2938; J. L. Sessler, E. Katayev, G. D. Pantos, P. Scherbakov, M. D. Reshetova, V. Khrustalev, V. M. Lynch, Y. A. Ustynyuk, *J. Am. Chem. Soc.* **2005**, *127*, 11442–11446; J. L. Sessler, J. M. Davis, *Acc. Chem. Res.* **2001**, *34*, 989–997.

[5] H. Z. Xie, S. Yi, X. P. Yang, S. K. Wu, *New J. Chem.* **1999**, *23*, 1105–1110. F. Werner, H.-J. Schneider, *Helv. Chim. Acta* **2000**, *83*, 465–478. M. J. Berrocal, A. Cruz, I. H. A. Badr, L. G. Bachas, *Anal. Chem.* **2000**, *72*, 5295–5299; B. H. M. Snellink-Ruël, M. M. G. Antonisse, J. F. J. Engbersen, P. Timmerman, D. N. Reinhoudt, *Eur. J. Org. Chem.* **2000**, 165–170; B. R. Linton, M. S. Goodman, E. Fan, S. A. Van Arman, A. D. Hamilton, *J. Org. Chem.* **2001**, *66*, 7313–7319; R. W. Hoffmann, F. Hettche, K. Harms, *Chem. Commun.* **2002**, 782–783; F. Hettche, P. Reiss, R. W. Hoffman, *Chem. Eur. J.* **2002**, *8*, 4946–4956; C. Lee, D. H. Lee, J.-I. Hong, *Tetrahedron Lett.* **2001**, *42*, 8665–8668; J. P. Clare, A. J. Ayling, J.-B. Joos, A. L. Sisson, G. Magro, M. N. Pérez-Payán, T. N. Lambert, R. Shukla, B. D. Smith, A. P. Davis, *J. Am. Chem. Soc.* **2005**, *127*, 10739–10746; D. R. Turner, M. J. Paterson, J. W. Steed, *J. Org. Chem.* **2006**, *71*, 1598–1608; F. Otón, A. Tárraga, A. Espinosa, M. D. Velasco, P. Molina, *J. Org. Chem.* **2006**, *71*, 4590- 4598; B. Schazmann, N. Alhashimy, D. Diamond, *J. Am. Chem. Soc.* **2006**, *128*, 8607–8614.

[6] B. P. Hay, T. K. Firman, *Inorg. Chem.* **2002**, *41*, 5502–5512; V. S. Bryantsev, B. P. Hay, *J. Am. Chem. Soc.* **2006**, *128*, 2035–2042.

[7] R. Custelcean, J. Bosano, P. V. Bonnesen, V. Kertesz, B. P. Hay, *Angew. Chem.* **2009**, *121*, 4085–4089; *Angew. Chem. Int. Ed.* **2009**, *48*, 4025–4029.

[8] R. Prohens, S. Tomàs, J. Morey, P. M. Deyà, P. Ballester, A. Costa, *Tetrahedron Lett.* **1998**, *39*, 1063–1066; R. Prohens, G. Martorell, P. Ballester, A. Costa, *Chem. Commun.* **2001**, 1456–1457; R. Prohens, M. C. Rotger, M. N. Piña, P. M. Deyà, J. Morey, P. Ballester, A. Costa, *Tetrahedron Lett.* **2001**, *42*, 4933–4936; A. Frontera, J. Morey, A. Oliver, M. N. Piña, D. Quiñonero, A. Costa, P. Ballester, P. M. Deyà, E. V. Anslyn, *J. Org. Chem.* **2006**, *71*, 7185–7195; M. N. Piña, C. Rotger, B. Soberats, P. Ballester, P. M. Deyà, A. Costa, *Chem. Commun.* **2007**, 963–965.

[9] C. Garau, A. Frontera, P. Ballester, D. Quiñonero, A. Costa, P. M. Deyà, *Eur. J. Org. Chem.* **2005**, 179–183; D. Quiñonero, A. Frontera, G. A. Suñer, J. Morey, A. Costa, P. Ballester, P. M. Deyà, *Chem. Phys. Lett.* **2000**, *326*, 247–254.

[10] D. Quiñonero, R. Prohens, C. Garau, A. Frontera, P. Ballester, A. Costa, P. M. Deyà, *Chem. Phys. Lett.* **2002**, *351*, 115–120; M. Neus Piña, M. C. Rotger, A. Costa, P. Ballester, P. M. Deyà, *Tetrahedron Lett.* **2004**, *45*, 3749–3752.

[11] G. Ambrosi, M. Formica, V. Fusi, L. Giorgi, A. Guerri, M. Micheloni, P. Paoli, R. Pontellini, P. Rossi, *Chem. Eur. J.* **2007**, *13*, 702–712.

[12] V. Ramalingam, M. E. Domaradzki, S. Jang, R. S. Muthyala, *Org. Lett.* **2008**, *10*, 3315–3318.

[13] M. Boiocchi, L. Del Boca, D. Esteban-Gómez, L. Fabbrizzi, M. Licchelli, E. Monzani, *J. Am. Chem. Soc.* **2004**, *126*, 16507–16514.

[14] G. A. Jeffrey, *An Introduction to Hydrogen Bonding*, Oxford Univerity Press, Oxford, **1997**.

[15] D. Quiñonero, C. Garau, C. Rotger, A. Frontera, P. Ballester, A. Costa, P. M. Deyà, *Angew. Chem.* **2002**, *114*, 3539–3542; *Angew.*

Chem. Int. Ed. **2002**, *41*, 3389–3392; M. Mascal, A. Armstrong, M. D. Bartberger, *J. Am. Chem. Soc.* **2002**, *124*, 6274–6276; I. Alkorta, I. Rozas, J. Elguero, *J. Am. Chem. Soc.* **2002**, *124*, 8593–8598; P. Gamez, T. J. Mooibroek, S. J. Teat, J. Reedijk, *Acc. Chem. Res.* **2007**, *40*, 435–444; O. B. Berryman, V. S. Bryantsev, D. P. Stay, D. W. Johnson, B. P. Hay, *J. Am. Chem. Soc.* **2007**, *129*, 48–58; T. J. Mooibroek, C. A. Black, P. Gamez, J. Reedijk, *Cryst. Growth Des.* **2008**, *8*, 1082–1093; T. J. Mooibroek, P. Gamez, J. Reedijk, *CrystEngComm* **2008**, *10*, 1501–1515; B. L. Schottel, H. T. Chifotides, K. R. Dunbar, *Chem. Soc. Rev.* **2008**, *37*, 68–83; J. Lu, J. K. Kochi, *Cryst. Growth Des.* **2009**, *9*, 291–296.

[16] A. Bondi, *J. Phys. Chem.* **1964**, *68*, 441–451.

[17] G. Ujaque, F. Maseras, O. Eisenstein, *Theor. Chem. Acc.* **1997**, *96*, 146–150.

[18] C. Estarellas, M. C. Rotger, M. Capó, D. Quiñonero, A. Frontera, A. Costa, P. M. Deyà, *Org. Lett.* **2009**, *11*, 1987–1990.

[19] P. Gans, A. Sabatini, A. Vacca, *Talanta* **1996**, *43*, 1739–1753; http://www.hyperquad.co.uk/index.htm, accessed 11 November, 2009.

[20] D. E. Gómez, L. Fabbrizzi, M. Licchelli, E. Monzani, *Org. Biomol. Chem.* **2005**, *3*, 1495–1500.

[21] M. J. Barrow, M. Currie, K. W. Muir, J. C. Speakman, D. N. J. White, *J. Chem. Soc. Perkin Trans. 2* **1975**, 15–18.

[22] F. P. Schmidtchen, M. Berger, *Chem. Rev.* **1997**, *97*, 1609–1646.

[23] H. Wamhoff, C. Bamberg, S. Herrmann, M. Nieger, *J. Org. Chem.* **1994**, *59*, 3985–3993.

[24] B. P. Hay, V. S. Bryantsev, *Chem. Commun.* **2008**, 2417–2428.

[25] C. Rotger, B. Soberats, D. Quiñonero, A. Frontera, P. Ballester, J. Benet-Buchholz, P. M. Deyà, A. Costa, *Eur. J. Org. Chem.* **2008**, 1864–1868.

[26] T. Steiner, *Angew. Chem.* **2002**, *114*, 50–80; *Angew. Chem. Int. Ed.* **2002**, *41*, 48–76.

[27] L. Alderighi, P. Gans, A. Ienco, D. Peters, A. Sabatini, A. Vacca, *Coord. Chem. Rev.* **1999**, *184*, 311–318; http://www.hyperquad.co.uk/hyss.htm, accessed 11 November 2009.

[28] L. J. Farrugia, *J. Appl. Crystallogr.* **1999**, *32*, 837–838.

[29] A. C. T. North, D. C. Phillips, F. S. Mathews, *Acta. Crystallogr. Sect. A* **1968**, *24*, 351–359.

[30] Bruker. SAINT Software Reference Manual, Version 6, Bruker AXS Inc., Madison, Wisconsin, **2003**.

[31] SADABS Siemens Area Detector Absorption Correction Program, G. M. Sheldrick, University of Göttingen, Göttingen, **1996**.

[32] A. Altomare, M. C. Burla, M. Camalli, G. L. Cascarano, C. Giacovazzo, A. Guagliardi, A. G. G. Moliterni, G. Polidori, R. Spagna, *J. Appl. Crystallogr.* **1999**, *32*, 115–119.

[33] SHELX97 Programs for Crystal Structure Analysis, G. M. Sheldrick, University of Göttingen, Göttingen, **1997**.

Received: November 20, 2009
Revised: January 14, 2010
Published online: March 10, 2010

